Kondo Decoherence: Finding the Right Spin Model for Iron Impurities in Gold and Silver

T. A. Costi,[1,2] L. Bergqvist,[1] A. Weichselbaum,[3] J. von Delft,[3] T. Micklitz,[4,7] A. Rosch,[4] P. Mavropoulos,[1,2] P. H. Dederichs,[1] F. Mallet,[5] L. Saminadayar,[5,6] and C. Bäuerle[5]

[1]*Institut für Festkörperforschung, Forschungszentrum Jülich, 52425 Jülich, Germany*
[2]*Institute for Advanced Simulation, Forschungszentrum Jülich, 52425 Jülich, Germany*
[3]*Physics Department, Arnold Sommerfeld Center for Theoretical Physics and Center for NanoScience, Ludwig-Maximilians-Universität München, 80333 München, Germany*
[4]*Institute for Theoretical Physics, University of Cologne, 50937 Cologne, Germany*
[5]*Institut Néel-CNRS and Université Joseph Fourier, 38042 Grenoble, France*
[6]*Institut Universitaire de France, 103 boulevard Saint-Michel, 75005 Paris, France*
[7]*Materials Science Division, Argonne National Laboratory, Argonne, Illinois 60439, USA*

(Received 8 October 2008; published 3 February 2009)

We exploit the decoherence of electrons due to magnetic impurities, studied via weak localization, to resolve a long-standing question concerning the classic Kondo systems of Fe impurities in the noble metals gold and silver: which Kondo-type model yields a realistic description of the relevant multiple bands, spin, and orbital degrees of freedom? Previous studies suggest a fully screened spin S Kondo model, but the value of S remained ambiguous. We perform density functional theory calculations that suggest $S = 3/2$. We also compare previous and new measurements of both the resistivity and decoherence rate in quasi-one-dimensional wires to numerical renormalization group predictions for $S = 1/2$, 1, and $3/2$, finding excellent agreement for $S = 3/2$.

DOI: 10.1103/PhysRevLett.102.056802 PACS numbers: 73.23.−b, 72.70.+m, 75.20.Hr

Introduction.—The Kondo effect of magnetic impurities in nonmagnetic metals, e.g., Mn, Fe, or Co in Cu, Ag, or Au, first manifested itself in the early 1930s as an anomalous rise in resistivity with decreasing temperature, leading to a resistivity minimum [1]. In 1964 Kondo explained this effect [2] as resulting from an antiferromagnetic exchange coupling between the spins of localized magnetic impurities and delocalized conduction electrons.

However, for many dilute magnetic alloys a fundamental question has remained unresolved to this day: which effective low-energy Kondo-type model yields a realistic description of the relevant multiple bands, spin, and orbital degrees of freedom [3]? Cases in point are Fe impurities in Au and Ag, the former being the very first magnetic alloy known to exhibit an anomalous resistivity minimum [1]. Previous attempts to fit experimental data on, for example, Fe impurities in Ag (abbreviated as AgFe) with exact theoretical results for thermodynamics, by assuming a fully screened low-energy effective Kondo model [4,5], have been inconclusive: specific heat data are absent and the local susceptibility of Fe in Ag obtained from Mössbauer spectroscopy [6] indicated a spin of $S = 3/2$ while a fully screened $S = 2$ model has been used to fit the temperature dependence of the local susceptibility [7].

A promising alternative route towards identifying the model for Fe in Au or Ag is offered by studying transport properties of high purity quasi-one-dimensional mesoscopic wires of Au and Ag, doped with a carefully controlled number of Fe impurities by means of ion implantation [8–13]. Magnetic impurities affect these in two different ways. Besides causing the aforementioned resistivity anomaly, they also make an anomalous contribution $\gamma_m(T)$ to the electronic phase decoherence rate $\gamma_\phi(T)$ measured in weak (anti)localization: an itinerant electron which spin flip scatters off a magnetic impurity, leaves a mark in the environment, and thereby suffers decoherence. By checking model predictions for both effects against experimental observations over several decades in temperature, decoherence can thus be harnessed as a highly sensitive probe of the actual form of the effective exchange coupling. Experiments along these lines [11,12] were consistent with a Kondo model in which the impurity spin is fully screened and inconsistent with underscreened or overscreened Kondo models [11]. A consistent description of both resistivity and decoherence measurements using the simplest fully screened Kondo model, the $S = 1/2$ single-channel Kondo model, was, however, not possible: different Kondo scales were required for fitting the resistivity and decoherence rates [11,12].

In this Letter we address the above problem via the following strategy. (i) We carry out density functional theory calculations within the local density approximation (LDA) for Fe in Au and Ag to obtain information that allows us to prescribe a low-energy effective model featuring three bands coupling to impurities with spin $S = 3/2$. (ii) We calculate the resistivity $\rho_m(T)$ and decoherence rate $\gamma_m(T)$ due to magnetic impurities for three fully screened Kondo models, with $n = 2S = 1$, 2, and 3, using Wilson's numerical renormalization group (NRG) approach. (iii) We compare these predictions to experimental data: extracting the characteristic Kondo temperature T_K^S for each choice of n from fits to $\rho_m(T)$ and using these T_K^S to obtain

parameter-free predictions for $\gamma_m(T)$, we find that the latter agree best with experiment for $n = 3$.

LDA calculations.—Fully relaxed density functional theory calculations employing the VASP code [14] showed that low-symmetry Fe configurations (split interstitials [15]) are energetically unfavorable: Fe impurities prefer an environment with cubic symmetry. As the calculated defect formation energy of an Fe interstitial was found to be about 2 eV higher than the energy of a substitutional defect, we discuss the latter case in the following. This is in line with experiments on Fe implantation in AgAu alloys, where only substitutional Fe-atoms are found [16].

Figure 1 shows the d-level local density of states of substitutional Fe in Ag and Au, obtained by spin-polarized calculations using a 108 atom supercell, with similar results being found for a 256 atom supercell. The cubic local symmetry leads to e_g (doublet) and t_{2g} (triplet) components with a e_g-t_{2g} splitting, $\Delta \gtrsim 0.15$ eV in LDA [Figs. 1(a) and 1(b)]. The widths Γ_{e_g} and $\Gamma_{t_{2g}}$ of the e_g and t_{2g} states close to the Fermi level (E_F) are of the order of 1 eV, resulting from a substantial coupling to the conduction electrons. The large t_{2g} component at E_F persists within LDA + U [Figs. 1(c) and 1(d)] using $U = 3$ eV and a Hund's coupling $J_H = 0.8$ eV.

The spin and orbital moments are given in the legends of Fig. 1 (spin-polarized Korringa-Kohn-Rostoker calculations yielded similar values [16]): Within spin-polarized LDA a large spin moment μ_S of approximately 3–$3.1\mu_B$ forms spontaneously, consistent with Mössbauer measurements that give 3.1–$3.2\mu_B$ for the spin moment for Fe in Ag [6]. In contrast, there is no tendency for a sizable orbital moment (or a Jahn-Teller distortion). The small orbital moments μ_L of $<0.1\mu_B$ (consistent with experimental results [17]) arise only due to weak spin-orbit coupling. We therefore conclude that the orbital degree of freedom is quenched on an energy scale set by the width $\Gamma_{t_{2g}}$ of the t_{2g} orbitals. Moreover, since the spin-orbit splitting of the localized spin in the cubic environment is proportional to μ_L^4, it is tiny, well below our numerical precision of 0.01 meV, and, therefore, smaller than the relevant Kondo temperatures.

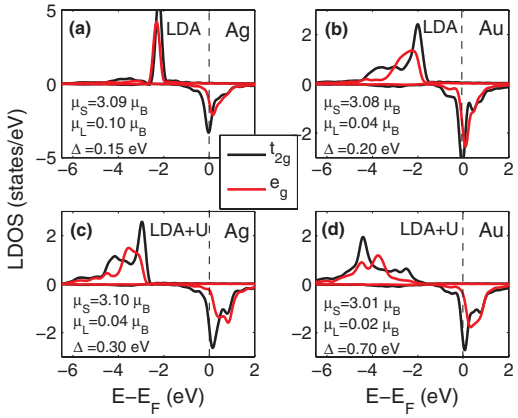

FIG. 1 (color online). The d-level local density of states (LDOS) of substitutional Fe in Ag and Au within spin-polarized LDA (a),(b) and LDA + U (c),(d), with inclusion of spin-orbit interactions, and showing the e_g [gray (red)] and t_{2g} (black) components of the d-level LDOS of FeAg (left-hand panels) and FeAu (right-hand panels). Majority (minority) contributions are shown positive (negative). Legends give the spin (μ_S) and orbital (μ_L) magnetic moments in units of the Bohr magneton μ_B and the splitting (Δ) between the e_g and t_{2g} components of the d-level LDOS.

Low-energy effective models.—The above results justify formulating an effective low-energy model in terms of the spin degree of freedom only. The large spin moment μ_S of 3–$3.1\mu_B$ suggests an effective spin $S = 3/2$. Our LDA results thus imply as effective model a spin-3/2 three-channel Kondo model, involving local and band electrons of t_{2g} symmetry. An alternative possibility, partially supported by the large (almost itinerant) t_{2g} component at E_F, would be to model the system as a spin 1 localized in the e_g orbitals, that is perfectly screened by two conduction electron channels of e_g symmetry. This spin is then also coupled to (almost itinerant) t_{2g} degrees of freedom via the ferromagnetic J_H. At high temperature, the latter binds an itinerant t_{2g} spin $1/2$ to the local spin 1 to yield an effective spin $3/2$, consistent with the spin moment of 3–$3.1\mu_B$ obtained within LDA, whereas in the low temperature limit, the irrelevance of J_H under renormalization [4] leads to the stated effective spin-1, two-band model. Though such a model is well justified only for $J_H \ll \Gamma_{t_{2g}}$, which is not the case here where $J_H \sim \Gamma_{t_{2g}}$, our LDA results do not completely exclude such a model. To identify which of the models is most appropriate, we shall confront their predictions with experimental data below.

We thus describe Fe in Ag and Au using the following fully screened Kondo model:

$$H = \sum_{k\alpha\alpha} \varepsilon_k c^\dagger_{k\alpha\sigma} c_{k\alpha\sigma} + J \sum_\alpha \mathbf{S} \cdot \mathbf{s}_\alpha. \qquad (1)$$

It describes n channels of conduction electrons with wave vector k, spin σ, and channel index α, whose spin density $\Sigma_\alpha \mathbf{s}_\alpha$ at the impurity site is coupled antiferromagnetically to an Fe impurity with spin $S = n/2$. Whereas our LDA results suggest $n = 3$, we shall also consider the cases $n = 1$ and 2.

NRG calculations.—The resistivity $\rho_m(T)$ and decoherence rate $\gamma_m(T)$ induced by magnetic impurities can be obtained from the temperature and frequency dependence of the impurity spectral density [18,19]. We have calculated these quantities using the NRG [20–22]. While such calculations are routine for $n = 1$ and 2 [21], they are challenging for $n = 3$. Exploiting recent advances in the NRG [20] we were able to obtain accurate results also for $n = 3$ (using a discretization parameter of $\Lambda = 2$ and retaining 4500 states per NRG iteration).

Figure 2 shows $\rho_m(T)$ and $\gamma_m(T)$ for $n = 2S = 1$, 2, and 3. For $T \gtrsim T_K^S$, enhanced spin-flip scattering causes both

$\rho_m(T)$ and $\gamma_m(T)$ to increase with decreasing temperature. For $T \lesssim T_K^S$ the effective exchange coupling becomes so strong that the impurity spins are fully screened by conduction electrons, forming spin singlets, causing $\rho_m(T)$ to saturate to a constant and $\gamma_m(T)$ to drop to zero. While these effects are well known [2,8–12], it is of central importance for this study that they depend quite significantly on $S = n/2$, in such a way that conduction electrons are scattered and decohered more strongly the larger the local spin S: With increasing S, (i) both resistivities and decoherence rates decay more slowly with T at large temperatures ($\gg T_K^S$), and (ii) the "plateau" near the maximum of $\gamma_m(T)$ increases slightly in maximum height $\gamma_m^{\max}$ and significantly in width. These changes turn out to be sufficient to identify the proper value of S when comparing to experiments below.

Comparison with experiment.—We compared our theoretical results for $\rho_m(T)$ and $\gamma_m(T)$ to measurements on quasi-one-dimensional, disordered wires, for two AgFe samples [11], (AgFe 2 and AgFe 3 having 27 ± 3 and 67.5 ± 7 ppm Fe impurities in Ag, respectively), with a Kondo scale $T_K \approx 5$ K (for $S = 3/2$, see below). These measurements extend up to $T \lesssim T_K$ allowing the region $T/T_K \lesssim 1$ of the scaling curves in Fig. 2 to be compared to experiment. At $T \gtrsim T_K \approx 5$ K (i.e., $T/T_K \geq 1$) the large phonon contribution to the decoherence rate prohibits reliable extraction of $\gamma_m(T)$ for our Ag samples (see below). In order to compare theory and experiment for temperatures $T/T_K \geq 1$, above the maximum in the decoherence rate, we therefore carried out new measurements on a sample (AuFe 3) with 7 ± 0.7 ppm Fe impurities in Au with a lower Kondo scale $T_K \approx 1.3$ K but, as discussed above, described by the same Kondo model. Combining both sets of measurement thereby allows a large part of the scaling curves in Fig. 2 to be compared with experiment.

Following [11], we subtract the electron-electron contribution [23] from the total resistivity ρ, yielding $\Delta\rho$ due to magnetic impurities (m) and phonons (ph):

$$\Delta\rho(T) = \rho_m(T) + \rho_{\rm ph}(T) + \delta. \quad (2)$$

Here δ is an (unknown) offset [24] and $\Delta\rho(T)$ is expressed per magnetic impurity. For temperatures low enough that $\rho_{\rm ph}(T)$ can be neglected, $\Delta\rho(T) - \delta$ corresponds to the theoretical curve $\rho_m(T) = \rho_m(0) f_S(T/T_K^S)$ (cf. caption of Fig. 2), where $\rho_m(0) = \Delta\rho(0) - \delta$ is the unitary Kondo resistivity. Figure 3 illustrates how we extract the Kondo scale T_K^S and $\rho_m(0)$ from the experimental data, by fitting the Kondo-dominated part of $\Delta\rho(T)$ in a fixed temperature range (specified in the caption of Fig. 3) to the NRG results of Fig. 2(a), using the ansatz

$$\Delta\rho(T) \approx \delta + [\Delta\rho(0) - \delta] f_S(T/T_K^S). \quad (3)$$

Such fits are made for each of the fully screened Kondo models, using T_K^S and δ as fit parameters. Importantly, the values for T_K^S and $\rho_m(0)$ obtained from the fits, given in the inset and caption of Fig. 3, respectively, show a significant S dependence: both T_K^S and $\rho_m(0)$ increase with S, since the slope of the logarithmic Kondo increase of the theory curves for ρ_m (cf. Fig. 2) decreases significantly in magni-

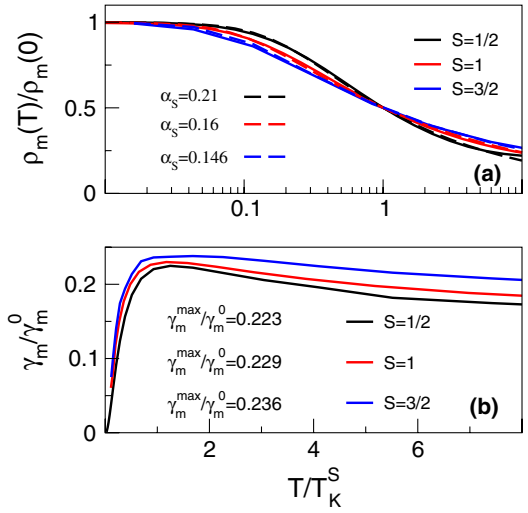

FIG. 2 (color online). (a) Resistivity $\rho_m(T)$ (solid lines) and (b) decoherence rate $\gamma_m(T)$ for $2S = n = 1, 2, 3$; $\rho_m(0) = 2\tau\bar{\rho}/\pi\hbar\nu_0$, $\gamma_m^0 = 2/\pi\hbar\nu_0$, where $\bar{\rho}$ is the residual resistivity, ν_0 the density of states per spin and channel, τ the elastic scattering time, and $\gamma_m^{\max}$ is the maximum value of $\gamma_m(T)$. We defined the Kondo scale T_K^S for each S via $\rho_m(T_K^S) = \rho_m(0)/2$. Dashed lines in (a) show that the empirical form $\rho_m(T)/\rho_m(0) \approx f_S(T/T_K^S)$ with $f_S(x) = [1 + (2^{1/\alpha_S} - 1)x^2]^{-\alpha_S}$, used to fit experimental to NRG results for $S = 1/2$ [25], also adequately fits the NRG results for $S = 1$ and $S = 3/2$.

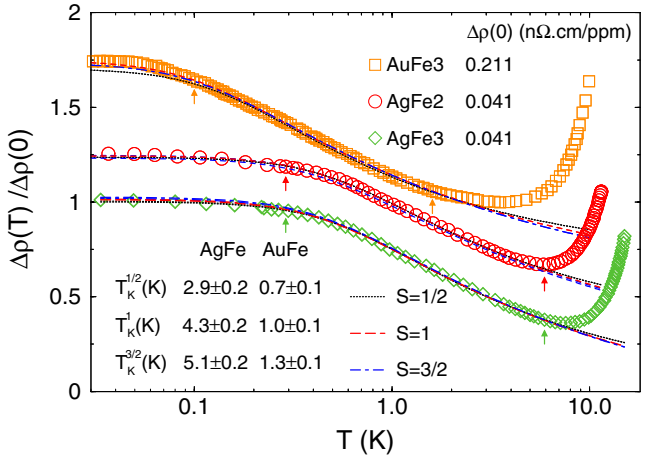

FIG. 3 (color online). Measured resistivities $\Delta\rho(T)$ (symbols) fitted to Eq. (3) (lines), for $n = 2S = 1$, 2, and 3, in the range below the onset of the phonon contribution, but above 100–200 mK [26]. Specifically, we used 0.1–1.6 K for AuFe and 0.29–5.9 K for AgFe (arrows). The curves for AgFe 2 and AuFe 3 have been offset vertically by 0.25 and 0.75, respectively. The inset gives the Kondo scales T_K^S for AgFe and AuFe extracted from the fits. Estimates of the unitary Kondo resistivities for $n = 1$, 2, and 3 (in units of $n\Omega \cdot$ cm/ppm) yield $\rho_m(0) = 0.041$, 0.047, and 0.049 for AgFe (averaged over the two samples) and 0.23, 0.26, and 0.27 for AuFe, respectively.

tude with S. Nevertheless, all three models fit the Kondo contribution very well, as shown in Fig. 3, so a determination of the appropriate model from resistivity data alone is not possible.

To break this impasse, we exploit the remarkably sensitive S dependence of the spin-flip-induced decoherence rate $\gamma_m(T)$. Figure 4 shows the measured dimensionless decoherence rate $\gamma_m(T)/\gamma_m^{\max}$ for Ag and Au samples (symbols) as function of T/T_K^S for $S = 1/2$, 1, and $3/2$, using the T_K^S values extracted from the resistivities, together with the corresponding parameter-free theoretical predictions (lines), taken from Fig. 2(b). The agreement between theory and experiment is poor for $S = 1/2$, better for $S = 1$, but excellent for $S = 3/2$, confirming the conclusion drawn above from *ab initio* calculations. The dependence on S is most strikingly revealed through the width of the plateau region (in units of T/T_K^S), which grows with S for the theory curves but shrinks with S for the experimental data (for which T_K^S grows with S), with $S = 3/2$ giving the best agreement.

Conclusions.—In this Letter we addressed one of the fundamental unresolved questions of Kondo physics: that of deriving and solving the effective low-energy Kondo model appropriate for a realistic description of Fe impurities in Au and Ag. Remarkably, for both Ag and Au samples, the use of a fully screened $S = 3/2$ three-channel Kondo model allows a quantitatively consistent description of both the resistivity and decoherence rate *with a single* T_K (for each material). Our results set a benchmark for the level of quantitative understanding attainable for the Kondo effect in real materials.

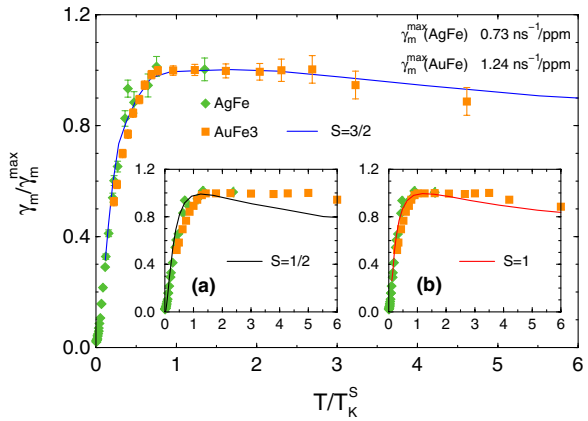

FIG. 4 (color online). Comparison of the measured (symbols) and theoretical (lines) results for the dimensionless decoherence rate $\gamma_m(T)/\gamma_m^{\max}$ as function of T/T_K^S, using $S = 3/2$. Insets show comparisons to $S = 1/2$ (a) and $S = 1$ (b). T_K^S for AgFe and AuFe was extracted from the resistivities (inset of Fig. 3), while $\gamma_m^{\max}$ was determined as the average plateau height in the region $T/T_K^{3/2} \in [0.7, 1.35]$. Typical error bars are shown for $S = 3/2$. They grow with increasing temperatures due to the increasing difficulty of subtracting the growing phonon contribution to the decoherence rate.

L. B. acknowledges support from the EU within the Marie Curie Actions for Human Resources and Mobility; P. M. from the ESF program SONS, Contract No. ERAS-CT-2003-980409; T. M. from the U.S. Department of Energy, Office of Science, Contract No. DE- AC02-06CH11357; L. S. and C. B. acknowledge technical support from the Quantronics group, Saclay, and A. D. Wieck and financial support from ANR PNANO "QuSPIN." Support from the John von Neumann Institute for Computing (Jülich), the DFG (SFB 608, SFB-TR12, and De730/3-2) and from the Cluster of Excellence Nanosystems Initiative Munich is gratefully acknowledged.

[1] W. J. de Haas, J. de Boer, and G. J. van den Berg, Physica (Amsterdam) **1**, 1115 (1934).
[2] J. Kondo, Prog. Theor. Phys. **32**, 37 (1964).
[3] P. Nozières and A. Blandin, J. Phys. (Paris) **41**, 193 (1980).
[4] A. C. Hewson, *The Kondo Problem to Heavy Fermions*, Cambridge Studies in Magnetism (Cambridge University Press, Cambridge, England, 1997).
[5] H. U. Desgranges, J. Phys. C **18**, 5481 (1985).
[6] P. Steiner and S. Hüfner, Phys. Rev. B **12**, 842 (1975).
[7] P. Schlottmann and P. D. Sacramento, Adv. Phys. **42**, 641 (1993).
[8] F. Pierre *et al.*, Phys. Rev. B **68**, 085413 (2003).
[9] F. Schopfer *et al.*, Phys. Rev. Lett. **90**, 056801 (2003).
[10] C. Bäuerle *et al.*, Phys. Rev. Lett. **95**, 266805 (2005).
[11] F. Mallet *et al.*, Phys. Rev. Lett. **97**, 226804 (2006).
[12] G. M. Alzoubi and N. O. Birge, Phys. Rev. Lett. **97**, 226803 (2006).
[13] T. Capron *et al.*, Phys. Rev. B **77**, 033102 (2008).
[14] G. Kresse and J. Furthmüller, Phys. Rev. B **54**, 11 169 (1996).
[15] G. Vogl, W. Mansel, and P. H. Dederichs, Phys. Rev. Lett. **36**, 1497 (1976).
[16] R. Kirsch *et al.*, Europhys. Lett. **59**, 430 (2002).
[17] W. D. Brewer *et al.*, Phys. Rev. Lett. **93**, 077205 (2004).
[18] T. Micklitz *et al.*, Phys. Rev. Lett. **96**, 226601 (2006).
[19] G. Zaránd *et al.*, Phys. Rev. Lett. **93**, 107204 (2004).
[20] A. Weichselbaum and J. von Delft, Phys. Rev. Lett. **99**, 076402 (2007).
[21] R. Bulla, T. A. Costi, and T. Pruschke, Rev. Mod. Phys. **80**, 395 (2008); T. A. Costi, A. C. Hewson, and V. Zlatić, J. Phys. Condens. Matter **6**, 2519 (1994);O. Sakai, Y. Shimizu, and N. Kaneko, Physica (Amsterdam) **186–188B**, 323 (1993).
[22] R. Peters, T. Pruschke, and F. B. Anders, Phys. Rev. B **74**, 245114 (2006); F. B. Anders and A. Schiller, Phys. Rev. Lett. **95**, 196801 (2005); W. Hofstetter, Phys. Rev. Lett. **85**, 1508 (2000); R. Bulla, A. C. Hewson, and Th. Pruschke, J. Phys. Condens. Matter **10**, 8365 (1998).
[23] B. L. Altshuler, A. G. Aronov, and D. E. Khmelnitzky, J. Phys. C **15**, 7367 (1982).
[24] Experiments measure resistance changes on ramping up the temperature, hence the unknown offset δ.
[25] D. Goldhaber-Gordon *et al.*, Phys. Rev. Lett. **81**, 5225 (1998).
[26] Below this temperature, the smaller signal to noise ratio makes the measurements less accurate.